doi:10.1016/j.jmb.2003.09.052 J. Mol. Biol. (2003) 334, 567–583

JMB

Available online at www.sciencedirect.com

SCIENCE DIRECT®

ELSEVIER

The Conserved Charged Residues of the C-terminal Region of FliG, a Rotor Component of the Na^+-driven Flagellar Motor

Professor Robert M. Macnab, who was professor of Yale University in the Department of Molecular Biophysics and Biochemistry, died on 7 September 2003 at 63 years old. This article is dedicated to him, a kind, gentle, fair, and unforgettable person

Tomohiro Yorimitsu, Atsushi Mimaki, Toshiharu Yakushi and Michio Homma*

Division of Biological Science Graduate School of Science Nagoya University, Chikusa-ku Nagoya 464-8602, Japan

*Corresponding author

FliG is an essential component of the flagellar motor and functions in flagellar assembly, torque generation and regulation of the direction of flagellar rotation. The five charged residues important for the rotation of the flagellar motor were identified in *Escherichia coli* FliG ($FliG^E$). These residues are clustered in the C terminus and are all conserved in $FliG^V$ of the Na^+-driven motor of *Vibrio alginolyticus* (Lys284, Arg301, Asp308, Asp309 and Arg317). To investigate the roles of these charged residues in the Na^+-driven motor, we cloned the *Vibrio fliG* gene and introduced single or multiple substitutions into the corresponding positions in $FliG^V$. $FliG^V$ with double Ala replacements in all possible combinations at these five conserved positions still retained significant motile ability, although some of the mutations completely eliminated the function of $FliG^E$. All of the triple mutants constructed in this study also remained motile. These results suggest that the important charged residues may be located in different places and the conserved charged residues are not so important for the Na^+-driven flagellar motor of *Vibrio*. The chimeric FliG protein ($FliG^{VE}$), composed of the N-terminal domain from *V. alginolyticus* and the C-terminal domain from *E. coli*, functions in *Vibrio* cells. The mutations of the charge residues of the C-terminal region in $FliG^{VE}$ affected swarming ability as in *E. coli*. Both the $FliG^V$ and the $FliG^{VE}$ proteins with the triple mutation were more susceptible to proteolysis than proteins without the mutation, suggesting that their conformations were altered.

Keywords: electrostatic interaction; flagellar motor; energy transduction; sodium type; *Vibrio*

Introduction

Bacterial flagella, which are filamentous organelles extending from the cell body, rotate reversibly by using the energy from the electrochemical potential of a specific ion, either H^+ or Na^+, across the cell membrane. The energy is harnessed by a motor complex that is located at the base of the flagellum. From studies of *Salmonella typhimurium* and *Escherichia coli*, which have H^+-driven flagellar motors, about 50 kinds of proteins are involved in flagellar assembly and function. Among them, only three proteins, MotA, MotB, and FliG, are

Present address: T. Yorimitsu, Department of Molecular, Cellular and Developmental Biology, University of Michigan, Ann Arbor, MI 48109, USA.

Abbreviations used: CCW, counter-clockwise; CW, clockwise; $FliG^E$, *E. coli* FliG; $FliG^V$, *V. alginolyticus* FliG; $FliG^{EV}$, *E. coli–V. alginolyticus* chimeric FliG; $FliG^{VE}$, *V. alginolyticus–E. coli* chimeric FliG; AAQQQ mutant, PomA mutant introduced R88A/K89A/E96Q/E97Q/E99Q substitutions; GFP, green fluorescent protein.

E-mail address of the corresponding author: g44416a@cc.nagoya-u.ac.jp

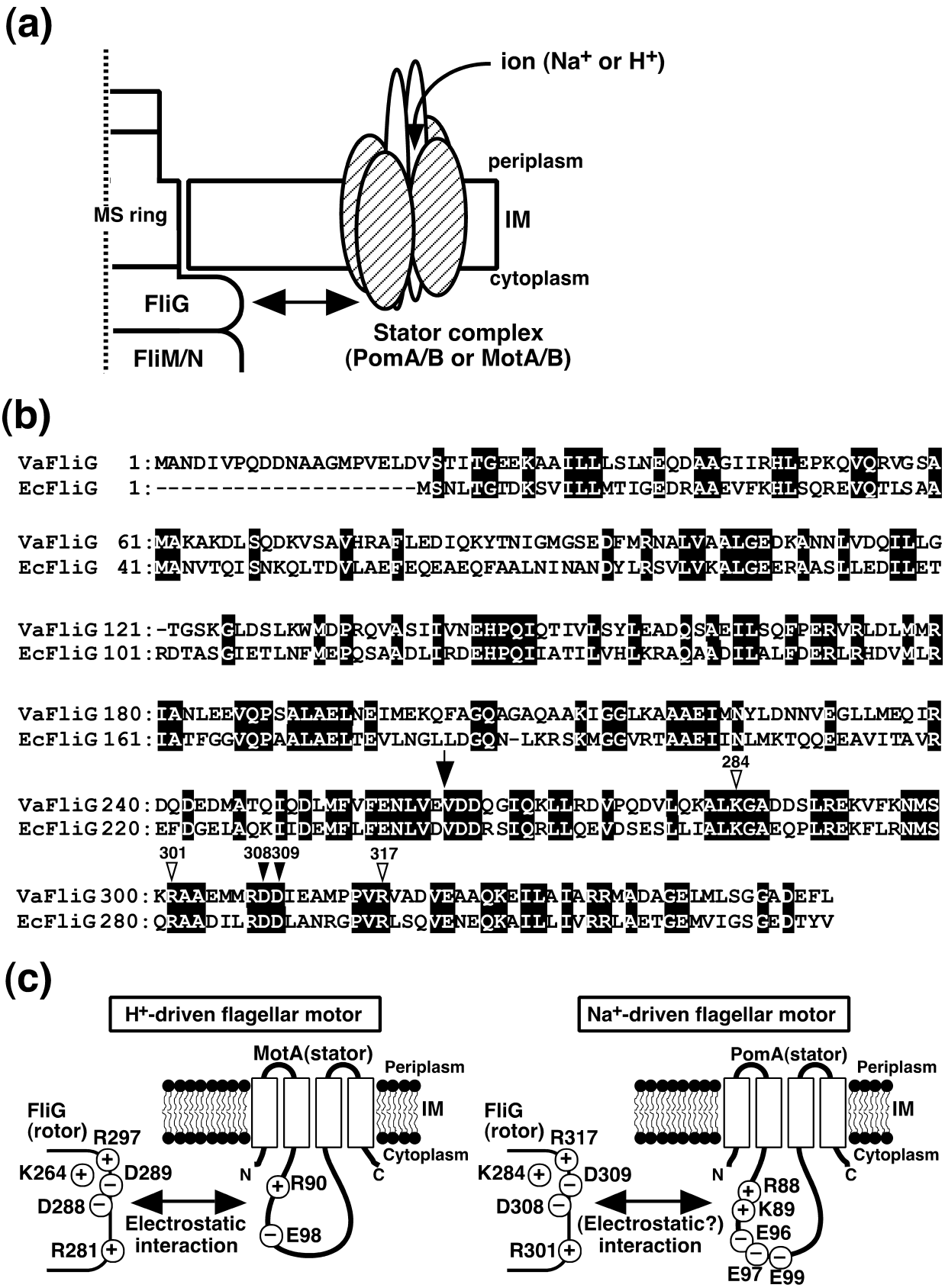

Figure 1. The stator and rotor components of the bacterial flagellar motor. (a) Schematic diagram of the flagellar motor. In the bacterial flagellar motor, the stator, which is composed of the PomA–PomB complex in the Na^+-driven flagellar motor (MotA–MotB complex in the H^+-driven flagellar motor), generates torque by the specific ion flux and transfers it to FliG of the rotor component. It is proposed that four PomA (MotA) and two PomB (MotB) form one unit of the complex.[34,37] (b) Alignment of the sequences of the rotor components, FliG of *V. alginolyticus* (VaFliG) and

thought to be directly involved in the energy conversion to generate the rotation from the ion flux.[1–3]

MotA and MotB, which are membrane-spanning proteins, form a H^+-channel complex. MotA has four transmembrane segments and a single large cytoplasmic loop, and MotB has a single transmembrane segment.[4,5] The C-terminal domain of MotB is believed to bind with the peptidoglycan layer[6,7] and fix the MotA–MotB complex as a stator around the basal body.[8] The MotA–MotB complex converts the H^+ flux into mechanical power for flagellar rotation.[9,10] It is thought that the ion flow induces the conformational changes of the complex and then changes the interactions between the cytoplasmic regions of MotA and FliG, which is a soluble protein, to drive the motor (Figure 1(a)).

FliG, FliM and FliN proteins are components of the switch complex, which has been genetically assigned, and together they form the C-ring structure identified by electron microscopy.[11,12] These three proteins are needed for flagellar assembly, torque generation, and regulation of the direction of flagellar rotation, counter-clockwise (CCW) or clockwise (CW).[13–15] Several lines of evidence indicate that FliG forms a ring structure 300 Å in diameter, which is composed of 25–40 copies, and is peripherally attached to the cytoplasmic side of the inner membrane by assembling with FliF, which forms the MS ring of the basal body[16–18] (Figure 1(a)). Among the motor components, the structure of FliG from the thermophile *Thermotoga maritima*, which possesses a flagellar motor whose ion specificity has not been determined, was resolved at atomic resolution and two crystal structures have been reported. One is the C-terminal domain (FliG-C) at 2.3 Å resolution[19] and the other is the middle and C-terminal domains (FliG-MC) at 2.8 Å resolution.[20]

It is known that some *Vibrio* species, *V. alginolyticus*, *V. parahaemolyticus*, and *V. cholerae*, and alkalophilic *Bacillus* species have Na^+-driven flagella.[21–25] In *Vibrio* species, PomA and PomB, homologs of MotA and MotB, respectively, are essential for the rotation of the flagellar motor. Like MotA and MotB, PomA and PomB have been shown to be functional partners. In the MotB or PomB component, a single negatively charged residue is conserved in the putative transmembrane segment and is suggested to be an ion-binding site.[26–28] The additional components MotX and MotY, which are specific for the *Vibrio* motor, are needed for torque generation.[29–32] They are localized to the outer membrane, although their functions are still unknown.[33] The PomA–PomB complex, when reconstituted into proteoliposomes, exhibited Na^+ uptake activity without MotX and MotY, but PomA alone did not. Because the molecular mass of the purified PomA–PomB complex was estimated to be 175 kDa by gel permeation chromatography, PomA and PomB are suggested to form a complex as oligomers, which might consist of four PomA and two PomB molecules[34] (Figure 1(a)). From the following lines of evidence, PomA is inferred to function as at least a dimer in the PomA–PomB complex: (i) PomA alone forms a stable dimmer;[34] (ii) a genetically fused tandem PomA dimer functions in the Na^+-type motor;[35] and (iii) when either one or both of the PomA subunits in the homodimer is mutated, the resulting complex is completely defective in motor function.[35] This inference is supported by cross-linking experiments using Cys-substituted mutants of PomA.[36] Recent systematic cross-linking analysis against the transmembrane segment of MotB also suggested that MotA and MotB are together oligomerized to work in the H^+-driven flagellar motor.[37]

Although the molecular mechanism of the flagellar motor is not yet clearly understood, several studies suggest that both the H^+-driven motor and the Na^+-driven motor use a common mechanism for torque generation. MotA of the H^+-type motor of *Rhodobacter sphaeroides* functions in *V. alginolyticus* cells as the Na^+-driven motor component.[38] In addition, MomB, a chimera between the N terminus of MotB from *R. sphaeroides* and the C terminus of PomB can functionally substitute for PomB in *V. alginolyticus* cells as a Na^+-driven motor.[39] A recent study also demonstrated that PotB, a chimera between the N terminus of PomB and the C terminus of MotB from *E. coli* constitutes the Na^+-driven motor together with PomA not only in *V. alginolyticus* but also in *E. coli* cells even in the absence of MotX or/and MotY.[40] Furthermore, Sowa *et al.*[41] analyzed the relationships between torque and speed in detail and concluded that characteristics are shared between the H^+-driven and Na^+-driven flagellar motors.

In the H^+-driven flagellar motor, a mechanical model for the interactions between MotA and FliG during motor rotation has been presented.[42] The residues in the cytoplasmic loop of MotA and the

of *E. coli* (EcFliG). White letters in black boxes indicate conserved residues between FliG of *V. alginolyticus* and of *E. coli*. The conserved charged residues mutagenized in this work are indicated by filled arrowheads (positively charged) and open arrowheads (negatively charged). The numbers over the arrowheads represent the positions of the amino acid residues in *V. alginolyticus* FliG. The arrow indicates the position of the junction in the chimeric FliG proteins between *V. alginolyticus* and *E. coli*. (c) Charged residues of the cytoplasmic loop of the stator part (PomA or MotA) and the C-terminal domain of the rotor part (FliG). Arg88 and Glu96 of PomA correspond to Arg90 and Glu98 of MotA, respectively. Charged residues, mutagenized here and previously, are suggested to be located at the interface between the stator and rotor parts.

C-terminal region of FliG were analyzed by mutagenesis, and the charged residues important for torque generation were identified to be Arg90 and Glu98 in MotA and Lys264, Arg281, Glu288, Glu289 and Arg297 in FliG[43,44] (Figure 1(c)). In the crystal structure of the *T. maritima* FliG, it is predicted that these charged residues are localized to the edges toward the outside of the FliG ring, and the electrostatic interactions that are exerted between the charged residues of MotA and FliG in the cytoplasmic regions cause motor rotation.[19,20] PomA shares two conserved charged residues in the cytoplasmic loop with MotA (Arg90 and Glu98, which correspond to Arg88 and Glu96 in PomA of *V. alginolyticus*), and has other charged residues, namely Lys89, Glu97 and Glu99, located near the two conserved residues (Figure 1(c)). When the charged residues of MotA are substituted with neutral residues, MotA completely eliminates motor rotation. On the other hand, substitutions of the charged residues, including the non-conserved residues of PomA do not affect the torque generation of the Na^+-driven flagellar motor.[45] This discrepancy has suggested that electrostatic interactions are not required for the rotation of the flagellar motor or that the other charged residues are involved in the electrostatic interactions of the Na^+-driven flagellar motor.

FliG in the H^+-driven motor of *E. coli* and the Na^+-driven motor of *V. alginolyticus* are more similar to each other than MotA and PomA. The five charged residues (Lys284, Arg308, Asp308, Asp309 and Arg317) identified to be important for *E. coli* flagellar rotation are all conserved in the *V. alginolyticus* FliG (Figure 1(b) and (c)). In the present work, we cloned and characterized the *fliG* gene of the polar flagellum of *V. alginolyticus*, and examined whether the conserved charged residues are involved in driving the Na^+-driven flagellar motor.

Results

Polar flagellar FliG of *V. alginolyticus*

To clone the *V. alginolyticus fliG* gene, we amplified the fragment containing *fliG* by PCR as described in Materials and Methods. The cloned *fliG* sequence of *V. alginolyticus* encodes 351 amino acid residues, and the predicted FliG protein has 40% amino acid sequence identity with the *E. coli* FliG protein (Figure 1(b)) and 96% and 86% identity with FliG from the related *Vibrio* species *V. parahaemolyticus* and *V. cholerae*, respectively.

To examine whether the cloned *fliG* gene functions for the polar flagellum, we tried to identify a *fliG* mutant from the laboratory stocks of Fla^- strains, which are derived from YM4,[46] a strain that posses the polar flagellum but has the defect of lateral flagella. One strain, NMB107, retained a swarm in the presence of arabinose only when transformed with the plasmid encoding the *fliG* gene under an arabinose-inducible promoter

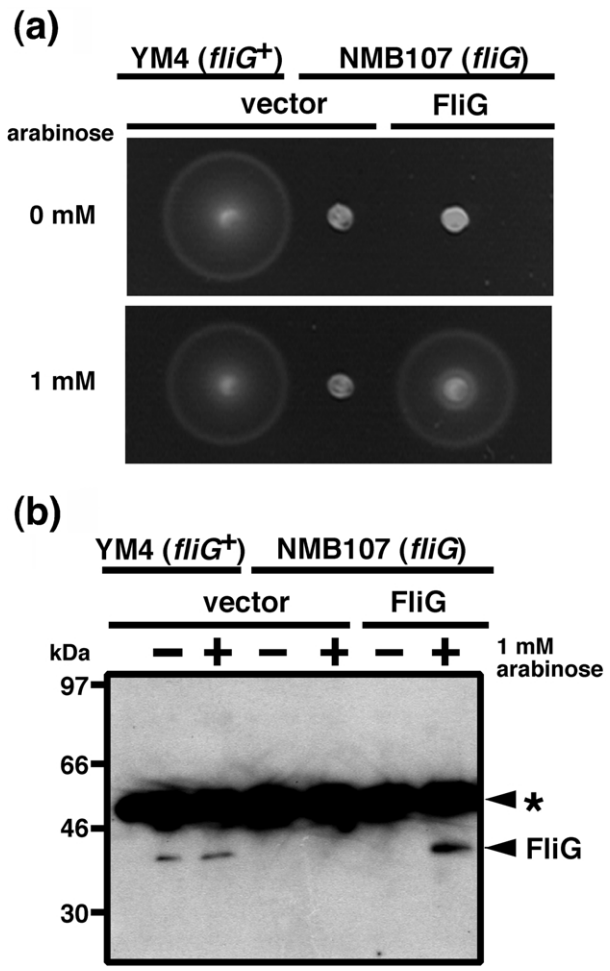

Figure 2. Expression of *fliG*. (a) Swarms of YM4 (*fliG*$^+$) or NMB107 (*fliG*$^-$) cells harboring a vector plasmid (pBAD33) or a plasmid encoding FliG (pTY101) under the control of the arabinose promoter on a 0.25% VPG plate in the absence (upper panel) or presence (lower panel) of 1 mM arabinose. (b) Detection of FliG proteins. YM4 or NMB107 cells harboring a vector plasmid or a plasmid encoding FliG were grown in the absence or presence of 1 mM arabinose, collected at mid-log phase and subjected to SDS-PAGE followed by immunoblotting with anti-FliG antibody. The asterisk indicates a non-specific band.

(Figure 2(a)). Although NMB107 cells have no flagella, after expression of *fliG* in the strain, the polar flagellum was easily observed by dark-field microscopy (data not shown). The site of the mutation in NMB107 was located at the codon for Arg135 (CGA) of *fliG*, which was altered to the opal codon (TGA).

To detect FliG protein by immunoblotting, we raised antibody against the synthetic peptide deduced from the amino acid sequence of FliG. Cells grown in the presence or absence of 1 mM arabinose were collected during log-phase and proteins were subjected to SDS-PAGE followed by immunoblotting with anti-FliG antibody (Figure 2(b)). In the presence of arabinose, the approximately 40 kDa FliG band (as estimated by

molecular markers) was observed with strain NMB107 harboring the plasmid carrying the *fliG* gene, and also independently with strain YM4 grown on arabinose. The molecular mass of FliG deduced from the amino acid sequence is 38,587 Da. FliG protein was not detected with NMB107 cells containing a vector control or the plasmid-borne *fliG* gene in the absence of arabinose, indicating that, as expected, NMB107 does not produce FliG protein due to the *fliG* mutation determined by sequence analysis.

Subcellular localization of GFP–FliG protein

To characterize the polar flagellar FliG protein of *V. alginolyticus*, we constructed green fluorescent protein (GFP)-fused FliG and expressed it under the control of an arabinose promoter in NMB107 cells. GFP was tagged to the N and C termini of FliG, and the proteins were designated GFP–FliG and FliG–GFP, respectively (Figure 3(a)). To examine whether these GFP-tagged FliG proteins are functional, we carried out swarm assays. Cells

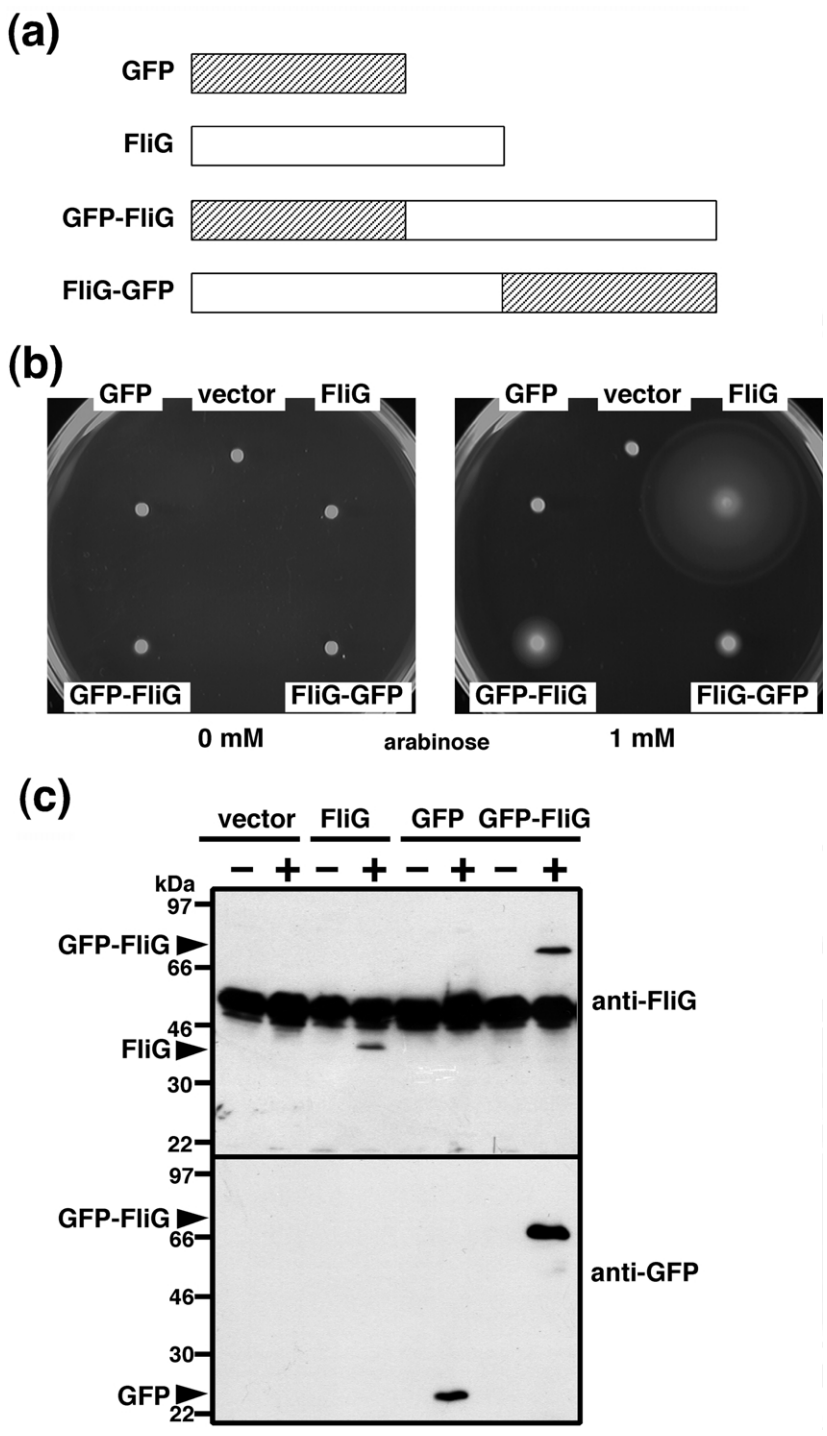

Figure 3. Fusion of FliG with GFP. (a) Diagram of the GFP-fused FliG proteins. Hatched boxes indicate the GFP sequence and open boxes indicate the FliG sequence. GFP was fused with the N and C termini of FliG, termed GFP–FliG and GFP–FliG, respectively. (b) Swarms of NMB107 cells harboring a vector plasmid (pBAD33) or a plasmid encoding FliG (pTY101), GFP (pTY200), GFP–FliG (pTY201) or FliG–GFP (pTY202) under the control of the arabinose promoter on 0.25% VPG plates in the absence (left panel) or presence (right panel) of 1 mM arabinose. (c) Detection of the GFP-fused FliG proteins. NMB107 cells harboring a vector plasmid or a plasmid encoding FliG, GFP or GFP–FliG were grown in the absence or presence of 1 mM arabinose, collected at mid-log phase and subjected to SDS-PAGE followed by immunoblotting with anti-FliG antibody (upper panel) or anti-GFP antibody (lower panel).

carrying both GFP–FliG and FliG–GFP were functional, but the swarm sizes were smaller than that made by cells carrying wild-type FliG. In addition, cells carrying GFP–FliG swarmed better than those carrying FliG–GFP (Figure 3(b)). By dark-field microscopy, the polar flagella were observed in cells with GFP–FliG or FliG–GFP as well as those with untagged FliG. Therefore, we used GFP–FliG for subsequent experiments.

To detect the GFP–FliG protein in cells, we carried out immunoblotting (Figure 3(c)). Immunoblot analysis with anti-FliG antibody or anti-GFP antibody showed that GFP–FliG was produced stably in NMB107 cells and no cleavage of the GFP moiety region was observed. These results suggest that GFP–FliG is functionally incorporated into the motor structure.

Next, we examined the subcellular localization of GFP–FliG in living cells (Figure 4). Cells harvested at mid-log phase were observed in a fluorescent microscope as described in Materials and Methods. A fluorescent dot was observed at the pole of NMB107 cells producing GFP–FliG, while no dot was observed in cells producing GFP (Figure 4(a); upper panels). Strain YM14 was previously isolated as an *rpoN* mutant and completely lacks the flagellar structure including the basal body.[47] There was no fluorescent dot at the pole of YM14 cells with GFP–FliG, as with GFP, and only dispersed fluorescence was seen (Figure 4(a); lower panels). To observe whether the fluorescent dot is co-located with the flagellar structure, we used a primary antibody against the polar flagellum and a second antibody coupled with rhodamine. As shown in Figure 4(b), a green dot of GFP–FliG co-localized with the red-staining flagellum at the same pole. Because the polar flagellum is covered with a lipid sheath connected to the outer membrane,[48] the cell body also seems to be stained. These results indicate that GFP–FliG is incorporated into the polar flagellar motor and functions in it.

Site-directed mutagenesis of individual charged residues

It has been reported that the five conserved charged residues located in the C-terminal region of FliG are functionally important for flagellar rotation of the H^+-driven flagellar motor of *E. coli* by electrostatically interacting with the charged residues of MotA[42–44] (Figure 1(c)). All five charged residues are conserved in the Na^+-driven motor of *V. alginolyticus* (Figure 1(b)). To study the role of the conserved charged residues of *V. alginolyticus* FliG, we replaced each of the charged residues with neutral amino acid residues. When substitutions with Ala were carried out, all of the mutant proteins were stably expressed in NMB107 cells (Figure 5(a)). The motility of cells expressing mutant FliG was examined by the swarm assay in a soft agar plate and the swimming speed in liquid containing 50 mM NaCl (Figure 5(a)). As shown for *E. coli* FliG mutants with single Ala substitutions, none of the single mutations with Ala severely affected swarm formation or swimming speed. The swarm size of the R301A and R317A mutants decreased to 73% and 61% of that of cells with wild-type FliG, respectively, but the swimming speeds were not affected.

A previous study of *E. coli* FliG showed that motility is more severely impaired by reversing the charges of some residues than by introducing neutral residues.[43] Therefore, we substituted residues with opposite charges, replacing the Lys284 residue with Glu, the Arg301 and Arg317 residues with Asp, or the Asp308 and Asp309 residues with Lys. FliG charge-reversed mutant proteins were produced as well as wild-type FliG (Figure 5(b)). The D289K mutation of *E. coli* FliG, which significantly impaired motility in *E. coli*, corresponded to the D309K mutation of *V. alginolyticus* FliG. However, cells expressing either D308K or D309K mutant FliG were capable of swarming and swimming as well as those expressing wild-type FliG (Figure 5(b)). The R301D mutant also swarmed, but the R281D mutant of *E. coli* FliG was non-motile. On the other hand, the K284E and R317D mutations caused more severe swarming defects in *V. alginolyticus* than the corresponding K264E and R297D FliG mutations in *E. coli*, respectively. In spite of the poor swarms made by the K284E and R301D mutants, these strains were able to swim as fast as the strain carrying wild-type FliG. Cells expressing the R317D mutant were never motile. The polar flagellum assembly in all the mutants was observed by dark-field microscopy and was similar to that of wild-type (results not shown).

Double substitutions of charged residues

It was reported previously that introduction of certain double mutations at positions of charged residues in *E. coli* FliG synergistically impairs the motor function.[43] To test this in *V. alginolyticus* FliG, we changed two of the five charged residues to Ala to generate ten double Ala-substituted mutants and also changed Asp308 and Asp309 into Asn residues (Figure 6). All of the double mutant proteins were stably produced in *Vibrio* cells (Figure 6, upper panel), and a normal polar flagellum was detected by microscopic observation in all of the mutant strains (results not shown). The swarming ability and the swimming speed of cells expressing FliG mutants with double substitutions were examined (Figure 6, lower panel). All of the double mutants have the ability to swim at a speed nearly comparable to that of the wild-type FliG. A slightly more severe swarming impairment was observed with cells expressing the mutants K284A/R301A, K284A/R317A, R301A/R317A or D309A/R317A than with those expressing each of singly Ala-substituted mutants. Similar to the phenotypes of the corresponding *E. coli* FliG mutants, a significant swarming ability was

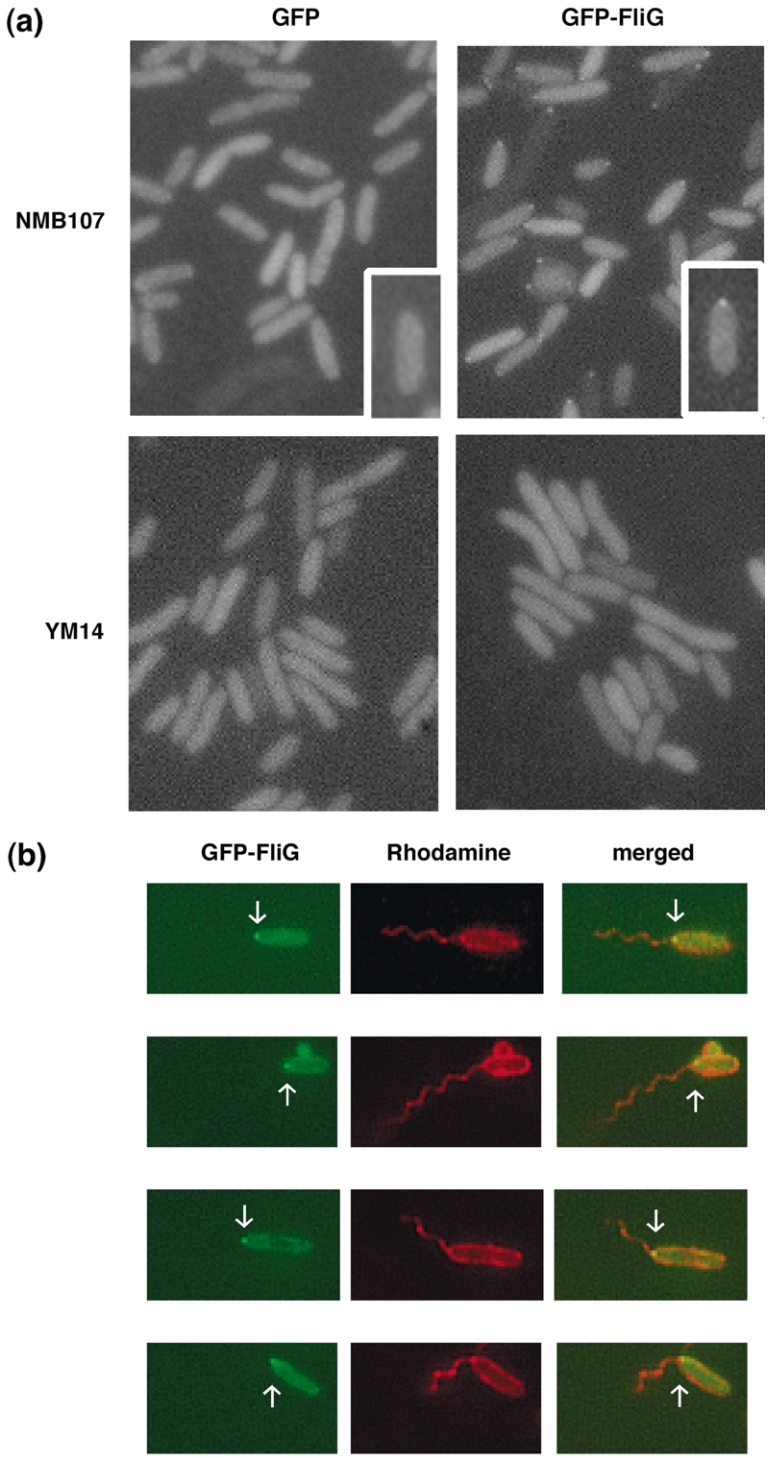

Figure 4. Subcellular localization of GFP–FliG. (a) NMB107 (upper panels) or YM14 (*rpoN*) (lower panels) cells harboring a plasmid encoding GFP (pTY200) (left) or GFP–FliG (pTY201) (right) were grown to mid-log phase in the presence of 1 mM arabinose and observed under a fluorescence microscope. (b) NMB107 cells expressing GFP–FliG grown to mid-log phase in the presence of 1 mM arabinose were treated with anti-polar flagella antibody followed by rhodamine-conjugated anti-rabbit IgG antibody and observed under a fluorescence microscope. Images of four independent cells are shown.

observed in cells with the K284A/D308A or K284A/D309A mutations in *V. alginolyticus* FliG. Five double mutants (R301A/D308A, R301A/D309A, D308A/D309A, D308A/R317A and D308N/D309N) were wild-type in their ability to swarm and swim, although the corresponding *E. coli* FliG double mutants were severely impaired in motility.

Triple substitutions of charged residues

The crystal structure of the C-terminal region of the *T. maritima* FliG reveals that the conserved charged residues are aligned in two individual lines, Lys266-Arg283-Asp290 and Arg283-Glu291-Arg299, suggesting that each combination has some role in the motor function.[19,20] To examine this in *V. alginolyticus* FliG, we constructed triple Ala mutants, K284A/R301A/D308A and R301A/D309A/R317A corresponding to the residues of *T. maritima* FliG. The protein production of the two triple mutants was similar to that of the wild-type FliG as detected by immunoblotting (Figure 7,

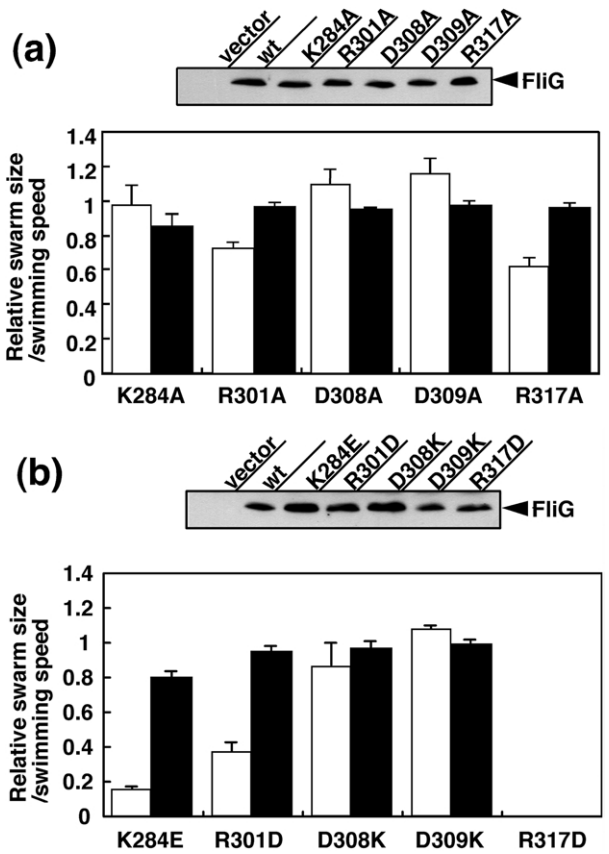

Figure 5. Effect of single substitutions of charged residues with an Ala residue on swarm formation and swimming speed (a) and of reversing charged residues (b). Detection of FliG mutant proteins (upper panel). NMB107 cells harboring a vector plasmid (pBAD33) or a plasmid encoding wild-type FliG or indicated FliG mutant (pTY101) were grown in the absence or presence of 1 mM arabinose, collected at mid-log phase and subjected to SDS-PAGE followed by immunoblotting with anti-FliG antibody. Swarm sizes and swimming speeds of the mutants with single substitution of charged residues (lower panel). Swarm diameters (open bars) and swimming speeds (filled bars) of NMB107 cells containing the various FliG mutants are shown in the histogram as a fraction of the swarm diameters and the swimming speeds of cells containing wild-type FliG. Swimming speeds in 50 mM NaCl were measured as described in Materials and Methods.

upper panel). Although both of the triple mutants remained motile, the swarm sizes of the K284A/R301A/D308A and R301A/D309A/R317A mutants were decreased to 28% and 5%, respectively, of that of a strain carrying wild-type FliG (Figure 7, lower panel). In liquid medium, the motile fraction of cells with the K284A/R301A/D308A mutation was similar to that of cells with wild-type FliG, while the number of motile cells in the R301A/D309A/R317A mutant population was very low (a small percentage of wild-type). We speculate that the motor rotation may be hard to be started by the mutant FliG. However, both of the triple mutants exhibited swimming speeds comparable to that of the wild-type strain.

Three other charged residues present in *E. coli* FliG (Arg281, Asp288 and Asp289) have been identified as a functionally important combination for flagellar rotation and are hypothesized to be minimally involved in the rotor–stator interaction.[42,43] We examined whether the equivalent triple Ala substitution (R301A/D308A/D309A) in the *V. alginolyticus* FliG affects motility (Figure 7). Although all possible combinations of double mutations of these three residues did not prevent motility, as shown in Figure 7, cells carrying the R301A/D308A/D309A triple mutant (produced at wild-type levels) swarmed poorly (20% of wild-type) but swam at the same speed as cells carrying the wild-type FliG. A triple mutant R301A/D308N/D309N was also constructed to minimize the effects of the substitutions of the Asp residues. The D308N/D309N double mutant exhibited completely normal swarming ability and swimming speed. The R301A/D308N/D309N mutation conferred a better swarming ability than the R301A/D308A/D309A mutation. When observed in the microscope, the flagellar formation of all of the triple mutants was similar to that of the wild-type strain.

Chimeras between FliG proteins derived from *V. alginolyticus* and from *E. coli*

It has been reported that chimeric proteins between *V. cholerae* and *E. coli* FliG have been constructed.[49] A chimera consisting of the N-terminal region of *V. cholerae* FliG fused to the C-terminal domain of *E. coli* FliG is able to function in the *V. cholerae fliG* null strain, but not the *E. coli* strain. The opposite *V. cholerae*–*E. coli* chimeric FliG also functioned in *E. coli* but not in *V. cholerae fliG*-deleted cells. We generated chimeric proteins between the *V. alginolyticus* and *E. coli* FliG proteins. A fusion FliG composed of the N-terminal portion of *V. alginolyticus* FliG and the C-terminal region of *E. coli* FliG was named $FliG^{VE}$ and the inverted fusion was designated $FliG^{EV}$ (Figure 8(a)). Swarm assays were carried out in the *fliG* mutant strains *V. alginolyticus* NMB107 and *E. coli* DFB225 (Figure 8(b)). NMB107 cells complemented by the $FliG^{VE}$ chimera swarmed as well as by wild-type *V. alginolyticus* FliG, but $FliG^{EV}$ did not complement. In contrast, *E. coli* FliG and the $FliG^{EV}$ chimera conferred the swarming ability to *E. coli* DFB225 cells, but $FliG^{VE}$ did not.

To further analyze the C-terminal region of FliG, we introduced mutations at the charged residues in the $FliG^{VE}$ chimera (Figure 8(c)). Such substitutions resulted in a loss of function in *E. coli* FliG but not in *V. alginolyticus* FliG. When the two residues Asp308 and Asp309 of $FliG^{VE}$ were replaced with the Asn residues, swarming ability was significantly decreased to 11% of the wild-type swarm size. The number of motile cells decreased significantly in the D308N/D309N mutant of $FliG^{VE}$, but had swimming speeds comparable to cells carrying $FliG^{V}$. Although the strain with

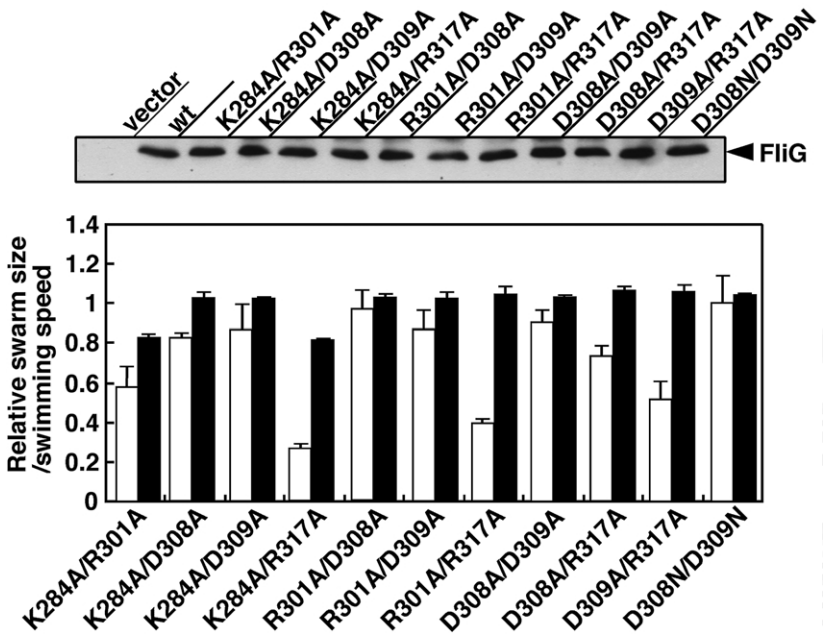

Figure 6. Effect of double substitutions of charged residues on swarm formation and swimming speed. Detection of FliG mutant proteins (upper panel). FliG mutant proteins were detected as described in the legend to Figure 5. Swarm sizes and swimming speeds of the mutants with the double substitutions of charged residues (lower panel).

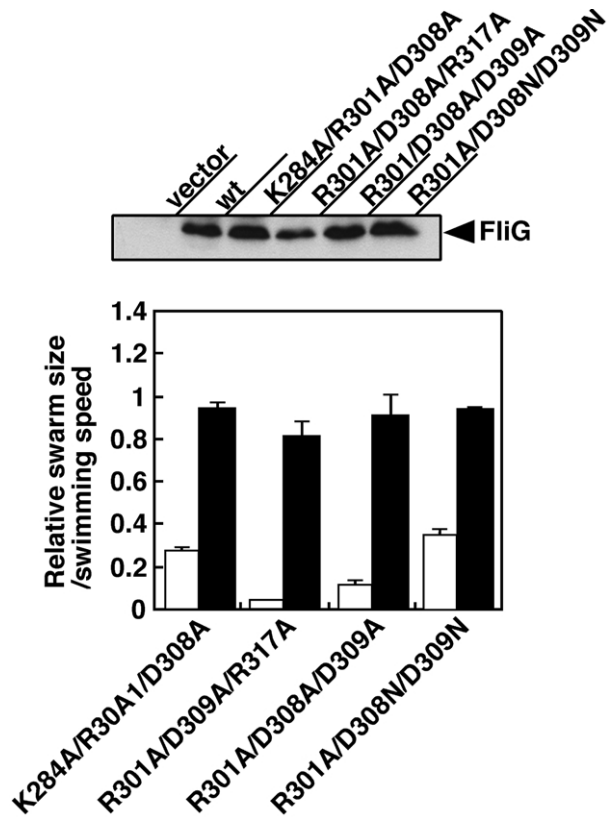

Figure 7. Effect of triple substitutions of charged residues on swarm formation and swimming speed. Detection of FliG mutant proteins (upper panel). FliG mutant proteins were detected as described in the legend to Figure 5. Swarm sizes and swimming speeds of the mutants with the triple substitutions of charged residues (lower panel).

FliG^{V} carrying the R301A/D308N/D309N triple mutation showed a 40% swarm ability compared to the wild-type, the introduction of the triple mutation into FliG^{VE} resulted in completely non-motile cells. The chimeric FliG^{VE} mutant proteins were produced in *Vibrio* cells at the same level as the intact FliG mutant proteins as determined by immunoblotting (Figure 8(d)), and the flagellation patterns observed by microscopy appeared to be normal (data not shown).

Effect of substitutions of charged residues on the proteolytic susceptibility of membrane-located FliG protein

In the flagellar motor, FliG is peripherally embedded in the cytoplasmic side of the membrane by assembling with FliF, which is a component of the basal body.[50] To confirm this, we cloned the *fliF* gene of *V. alginolyticus* and co-produced the *V. alginolyticus* FliG and FliF in *E. coli* cells. In the absence of FliF co-production, the FliG protein was detected only in the supernatant fraction after high-speed centrifugation. In contrast, when expressed with FliF, FliG was predominantly pelleted in the membrane fraction (Figure 9(a)). To examine whether co-expression of PomA and PomB affects the protease susceptibility of FliG, we prepared membrane vesicles from cells expressing FliF and FliG with or without PomA and PomB and treated them with the proteases, proteinase K and trypsin. As shown in Figure 9(b), without co-expression of PomA and PomB, FliG proteins were degraded by both proteases more significantly than those with PomA and PomB, indicating that PomA and PomB affect the protease sensitivity of membrane-localized FliG.

We next examined whether introduction of mutations into the charged residues of FliG^{V} and

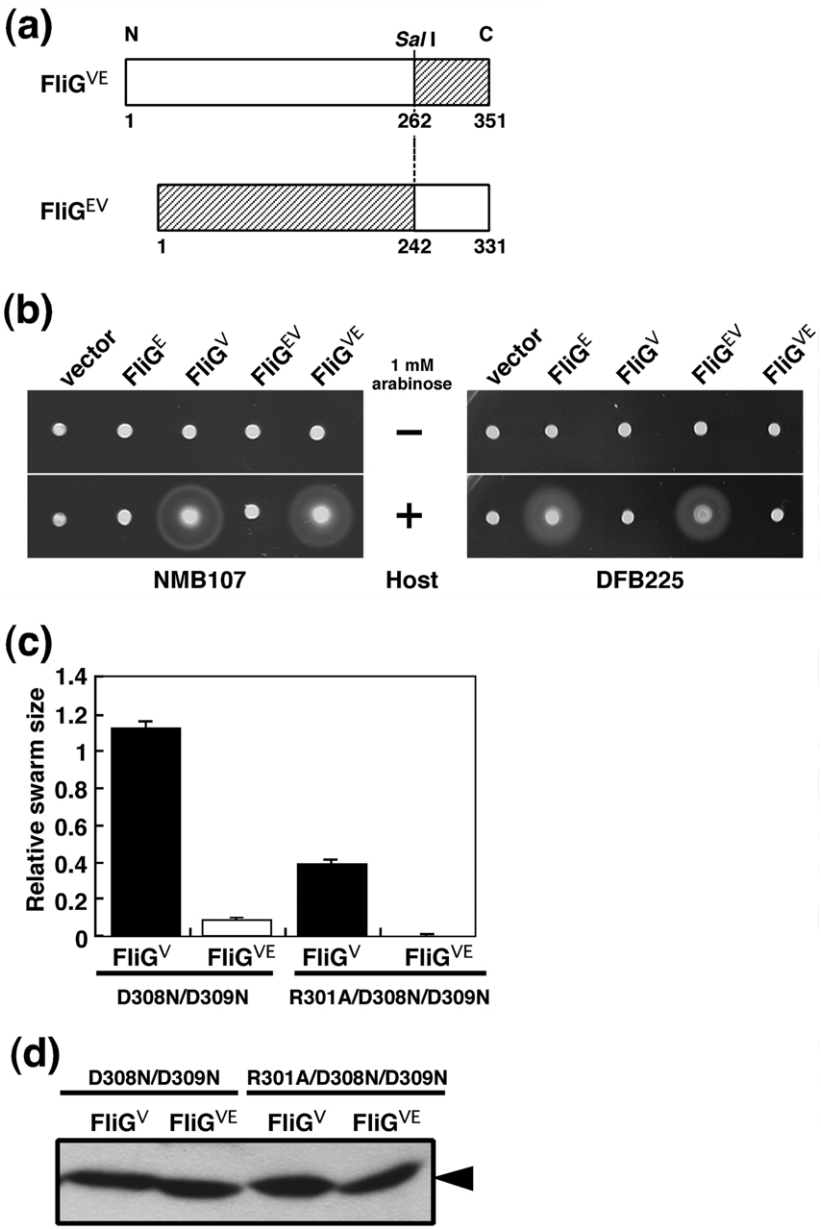

Figure 8. Characterization of chimeric FliG. (a) Schematic diagrams of chimeric FliG proteins. Chimeric proteins FliG^{VE} and FliG^{EV} were constructed as described in Materials and Methods. White boxes indicate the *V. alginolyticus* FliG-derived sequence and hatched boxes indicate the *E. coli* FliG sequence. Numbers correspond to the amino acid residues. (b) Complementation by chimeric FliG proteins. DFB225 or NMB107 cells expressing the FliG proteins were cultured overnight and spotted on a TB or VPG 0.25% agar plate containing chloramphenicol in the presence or absence of 1 mM arabinose. FliG^{E} and FliG^{V} indicate FliG derived from *E. coli* FliG and from *V. alginolyticus*, respectively. (c) Swarm profiles of the chimeric FliG^{VE} mutants. Swarm diameters of NMB107 cells containing FliG^{V} or FliG^{VE} with D308N/D309N or R301A/D308N/D309N mutations are shown in the histogram as a fraction of the swarm diameters of cells with the wild-type FliG. (d) Detection of chimeric FliG^{VE} mutant proteins. FliG and FliG^{VE} mutant proteins were detected by immunoblotting as described in the legend to Figure 5.

FliG^{VE} affects the protease susceptibility of these proteins (Figure 9(c)). FliG^{V} proteins with the D308N/D309N substitution, which does not affect the motility as shown above, exhibited a susceptibility equivalent to the wild-type FliG^{V}. However, the R301A/D308N/D309N triple mutant, which caused reduced swarming to less than 40% of wild-type, showed an increased susceptibility to proteolysis. The susceptibility to proteases was also examined with the chimeric FliG^{VE} proteins. The FliG^{VE} protein without substitutions was slightly more susceptible to proteolysis than FliG^{V} protein. As shown with the FliG proteins, the D308N/D309N-mutagenized FliG^{VE} protein was digested to the same level as the FliG^{VE} protein without substitutions and the R301A/D308N/D309N-mutagenized FliG^{VE} protein was slightly more digested than FliG^{VE} protein.

Discussion

FliG has multiple roles in the operation of the flagellar motor, the flagellar architecture, torque generation and the clockwise (CW) to counterclockwise (CCW) rotational switch.[13,15,51] In this work we first cloned the *fliG* gene for the polar flagellum of *V. alginolyticus* and carried out a basic characterization. Based on previous biochemical and structural evidence, it is known that FliG forms a switch complex with FliM and FliN.[11,12,52] Kubori *et al*.[50] have reported that only FliF is needed for FliG localization, but FliM and FliN are not. Sourjik & Berg[53] observed the assembly of FliM–YFP (FliM fused with yellow fluorescent protein which is a variant of GFP) on the switch complex in *E. coli* cells and found that FliM–YFP localization was dependent on FliG but independent

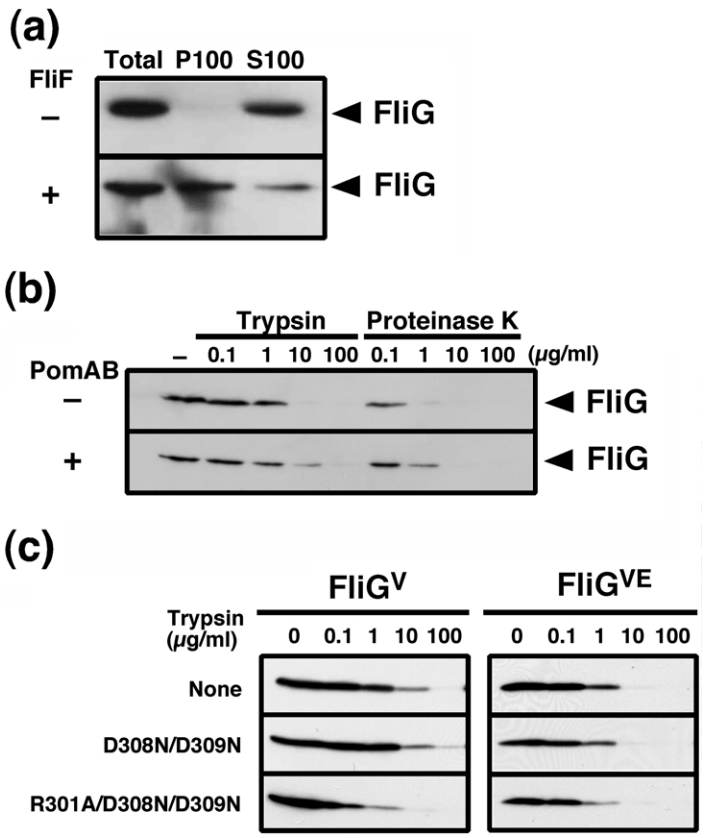

Figure 9. Localization and protease sensitivity of FliG proteins. (a) Localization was examined during co-expression of FliG with FliF. Cell suspensions of JM109 cells harboring plasmids carrying FliG alone (pTY101) or FliG with FliF (pTY601) were passed through a French press, and cytoplasm (S100) and membrane (P100) fractions were prepared from the lysates (Total) by centrifugation as described in Materials and Methods. Immunoblotting was carried out with anti-FliG antibody. (b) Effect of co-expression of PomA and PomB on the protease susceptibility of membrane-associated FliG. Membrane vesicles of JM109 cells harboring a plasmid carrying *V. alginolyticus* FliF and FliG^{V} (pTY601) with or without plasmids carrying PomA and PomB (pJN131) were treated with trypsin or proteinase K at the indicated concentrations, or without protease (−). (c) Effect of mutations of charged residues on protease susceptibility of FliG or the FliG^{VE} chimera. Membrane vesicles of JM109 cells harboring plasmids carrying *fliF* and *fliG*^{V} (pTY601) (left panel) or a FliG^{VE} chimera (pTY602) (right panel), with or without the indicated mutations shown on the left side, together with the plasmid carrying PomA and PomB (pJN131) were treated with trypsin at the indicated concentrations. None indicates the wild-type. Immunoblotting was carried out with anti-FliG antibody.

of FliN. It is known that the direction of flagellar rotation is regulated by phosphorylation or dephosphorylation of CheY and that phospho-CheY binds to FliM of the switch complex to change the direction of rotation from CCW to CW.[54–57]

Here, we were able to observe the assembly of GFP-fused FliG (GFP–FliG) in the polar flagellar structure in living *Vibrio* cells. The present work showed that FliG localization is not observed in an *rpoN* strain, which does not synthesize flagella.[47] We have cloned the *fliF* gene of the polar flagellum of *V. alginolyticus*, which functionally complemented the Δ*fliF* strain, NMB196, generated from the lateral-flagella-defective strain VIO5. The localization of GFP–FliG in the membrane of *E. coli* cells was observed only when expressed together with *V. alginolyticus* FliF (data not shown), and the interaction between FliF and FliG was shown by our biochemical analysis. These results are in agreement with the previous results for *E. coli* and *S. typhimurium* as described above, suggesting that the mechanism for the assembly of the components in the switch complex is basically shared between peritrichous and polar-flagellated cells. The functional GFP–FliG should be a useful tool for studying the mechanism of flagellar assembly.

For the flagellar motor rotation, the stator portion (the PomA–PomB complex for the Na^+-type and the MotA–MotB complex for H^+-type) converts the ion flux generated by the electrochemical potential into mechanical energy and transfers it to the rotor portion (FliG) (Figure 1(a)). In the H^+-driven flagellar motor, it has been proposed that the charged residues in the C-terminal domain of the rotor protein FliG and in the cytoplasmic loop of the stator protein MotA have a role in the electrostatic interaction, which is a functionally important event for the motor rotation[42] (Figure 1(c)). Those residues in the H^+-driven components are conserved in the Na^+-driven components (Figure 1(c)). However, we have demonstrated that these charged residues are not essential for motor rotation, suggesting that the stator component (PomA) of the Na^+-driven motor of *V. alginolyticus* has extra or additional essential charged residues, or alternatively, that the specific charge interaction is not as important in the Na^+-driven motor.[45] Several studies suggest that the mechanism of torque generation in the Na^+ and H^+-type motors is shared. *Rhodobacter sphaeroides* MotA, which is the H^+-driven motor component, functions in *pomA*-defective *Vibrio* cells as a component of the Na^+-type motor.[38] The *V. cholerae*–*E. coli* FliG fusion,[49] the chimera FliG^{VE}, is functional in *V. cholerae* and a similar result was obtained in this study using *V. alginolyticus*. It has been shown that PomA and PotB (a chimera of *V. alginolyticus* PomB and *E. coli* MotB) can function with *E. coli* FliG in *E. coli* cells

and the *E. coli* flagellar motor can rotate using the Na^+ flux in the absence of MotX or/and MotY.[40]

When amino acid sequences of *V. alginolyticus* FliG and *E. coli* FliG are aligned, their C-terminal regions have much higher homology than the cytoplasmic loops of PomA and MotA. We focused on the five conserved charged residues Lys284, Arg301, Glu308, Glu309 and Arg317 of *V. alginolyticus* FliG that correspond to the *E. coli* FliG residues predicted to be crucial for function.[43] When the *E. coli* FliG was mutagenized, some conserved charged residues affected the motor rotation synergistically. In *V. alginolyticus* FliG, not only single, but also multiple substitutions with neutral residues did not affect torque generation, although the swarming ability of the strains was somewhat decreased. These results suggest that these conserved residues of *V. alginolyticus* FliG are not essential for rotating the Na^+-driven motor but are involved in controlling the direction of the rotation of the flagellar motor. From the crystal structure of the *T. maritima* FliG, that can function in *E. coli*, a subset of three of the five key charged residues can be linearized in two individual arrangements and each set of arrangements is speculated to make the torque for one direction, CCW or CW.[19,20] We triply mutagenized the residues corresponding to each of the combinations of *T. maritima* FliG. Cells with either of the triple mutants were poor swarmers, but they were able to swim at speeds comparable to cells with wild-type FliG. Conformational changes in FliG might induce the change between CCW and CW state of the flagellar rotation or might affect the force generation of the motor in response to increasing load.

When the three residues Arg301, Asp308 and Asp309 of *V. alginolyticus* FliG were neutralized (the R301A/D308N/D309N mutant), the triple mutants still retained motility. Triple mutations of the equivalent three residues, Arg281, Asp288 and Asp289 in *E. coli* FliG resulted in a complete loss of function and were suggested to be primarily important for electrostatic interactions in *E. coli*.[43] To exclude the possibility that misreading of the opal mutation in the *fliG* gene in strain NMB107 (which was used as the *fliG* mutant in this work) results in the production of some functional protein, we generated a *fliG* deletion mutant, NMB198. When the mutant FliG proteins were expressed in NMB198, we obtained the same results as with NMB107 (data not shown). Based on these lines of evidence in FliG and PomA of *V. alginolyticus*, we may infer that electrostatic interactions are not required, or at least are not important, for the rotation of the Na^+-driven motor. However, it is highly possible that other subsets of charged residues that are not shared with *E. coli* FliG, are located in the C-terminal domain of *V. alginolyticus* FliG and are involved in the Na^+-driven motor. The candidates may be the charged residues K300 and E311, which are predicted to locate on the same surface of the conserved residues. To clarify the roles of charged residues in *V. alginolyticus*, the interaction of the charged residues between PomA and FliG should be investigated.

Proteolysis analysis showed that co-expression of PomA and PomB affects the protease sensitivity of FliG. We speculate that the PomA–PomB complex directly blocks the proteolysis of FliG protein or alters the FliG conformation because of their physical interaction. Either $FliG^V$ or $FliG^{VE}$ (the chimera between the N-terminal region of *V. alginolyticus* FliG and the C-terminal region of *E. coli* FliG) with the R301A/D308N/D309N substitution is less resistant to proteolysis than the wild-type proteins or the D308N/D309N mutant proteins. This protease susceptibility of the mutant proteins has also been observed in the *E. coli* FliG mutants.[43] We speculate that the charged residues are required for sustaining the functional structure, and the conformational changes caused by the multiple mutations are enough to impair FliG function or the functional (electrostatic) interaction with the stator.

In the present mutational study of the *V. alginolyticus* FliG, the R317D mutant was the only nonfunctional FliG. Double and triple mutants combined with the Ala mutation of the Arg317 residue decreased the function more severely than the other mutations. According to these results, the Arg317 residue could be one of the candidates for a functionally important charged residue in the Na^+-driven flagellar motor. The corresponding residue of *E. coli* FliG, Arg297, which is located between helix 5 and helix 6 as deduced from the crystal structure of *T. maritima* FliG,[19,20] is found to be moderately important for function.[43] There are also other possible candidates in the C-terminal segment of *V. alginolyticus* FliG, which contains three basic and four acidic residues. Further studies are needed to identify the essential residues for the Na^+-driven flagellar motor if those residues do exist. The flagellar motor is likely to contain 25–40 copies of FliG, which are assembled in a ring-shaped structure and attach to the MS-ring directly.[16–18] The predicted stoichiometry of PomA and PomB or MotA and MotB in the complex is 4:2, so the PomA–PomB (MotA–MotB) complex has four cytoplasmic loops, of which the charged residues are predicted to interact with the charged residues of the C-terminal FliG (Figure 1(a)). At this time, it is difficult to predict the functional contacts exerted between the cytoplasmic regions of FliG and PomA.

It has been reported that the CW–CCW switching of *Vibrio* cells is abnormal in the Na^+-driven motor composed of the *R. sphaeroides* wild-type MotA or of the quadruple-mutant form of PomA (AAQQQ mutant).[38,45] Some of the FliG mutants described here also showed a discrepancy between the swarm and swimming speed, which is often seen in chemotaxis mutants. It is hypothesized that the rotor–stator interface is first aligned correctly by the electrostatic interaction, and this alignment is a trigger for the following torque-generating events.

It is easy to speculate that the stator–rotor arrangement affects CW–CCW switching. Such a system of regulating the rotation by electrostatic interactions has been proposed for the F_1-ATPase, which is also known to be a rotary motor.[58] The β subunit of F_1-ATPase has a conserved acidic motif, the DELSEED motif, which was assumed to contact the γ subunit and to be involved in torque generation. However, Ala-scanning mutagenesis of the DELSEED motif in the thermophilic *Bacillus* PS3 F_1-ATPase showed that all of examined mutants rotate with as much torque as wild-type.[59] However, the ε subunit of F_1-ATPase, an intrinsic inhibitor of the enzyme, is unable to inhibit the ATPase activity in the DELSEED mutants,[60] indicating that the DELSEED motif does not have a direct role in torque generation, but that the electrostatic interactions with the ε subunit function to exert the inhibitory activity. Further, it has been suggested that the ε subunit of the F_1F_o-ATP synthase regulates the switch between the ATP hydrolysis mode and the ATP synthase mode largely by changing conformation, which might regulate the direction of the rotation of the enzyme.[61]

In the H^+-driven flagellar motor, one model for the motor rotation coupling with H^+ flow has been presented as follows.[62] (i) In the stator, MotB has an Asp32 residue in an ion-binding site in a transmembrane segment. However, a channel of the MotA–MotB complex is not opened and H^+ is not accessible to the binding site. (ii) A conformational change of the stator involving the Pro173 residue causes a gate to open in the channel, which is induced by an electrostatic interaction between the rotor and the stator. (iii) H^+ can enter the channel from the periplasm and bind to Asp32. (iv) The binding of H^+ triggers a further conformational change to drive the rotor movement and then H^+ is released into the cytoplasm. (v) The rotor moves farther and the stator returns to the first conformation. This model could be applied basically to the Na^+-driven motor, because the two Pro residues, Pro173 and Pro222, in the *E. coli* model are conserved in PomA (Pro153 and Pro199, respectively). The Asp32 residue of MotB is conserved in PomB. Asp24 is the only charged residue in the transmembrane segment of PomB and substitution of that residue causes cells to become non-motile. However, a mutant PomA with a substitution at Pro199 was unable to associate with PomB, suggesting that unlike Pro222 of MotA, Pro199 may play a role in forming or stabilizing the PomA–PomB complex.[35] It seems that electrostatic interactions are not important for the rotation of the Na^+-driven motor, so the conformational changes that cause the opening of the gate might be unnecessary for the Na^+-driven motor. Ions might pass more effectively through the channel of the Na^+-driven flagellar motor, which could confer a much higher rotational speed on the Na^+-driven flagellar motor than the H^+-driven motor (1700 rps *versus* 300 rps, respectively).[63,64]

Materials and Methods

Bacterial strains, plasmids, growth conditions and media

The bacterial strains and plasmids used in this study are listed in Table 1. *V. alginolyticus* cells were cultured at 30 °C in VC medium (0.5% (w/v) polypeptone, 0.5% (w/v) yeast extract, 0.4% (w/v) K_2HPO_4, 3% (w/v) NaCl, 0.2% (w/v) glucose) or VPG medium (1% (w/v) polypeptone, 0.4% (w/v) K_2HPO_4, 3% (w/v) NaCl, 0.5% (w/v) glycerol). For the swarm assay, overnight cultures of cells were spotted onto 0.25% (w/v) agar-VPG plates containing 2.5 μg/ml of chloramphenicol and incubated at 30 °C. *E. coli* cells were cultured 30 °C in TB medium (1% (w/v) tryptone, 0.3% (w/v) NaCl) and overnight cultures of cells were spotted onto 0.25% agar-TB plates containing 25 μg/ml of chloramphenicol and incubated at 30 °C. If necessary, L-arabinose was added to a final concentration of 1 mM.

Routine DNA manipulations were carried out according to standard procedures.[65] Plasmid pSU41 carries the *lac* promoter.[66] Plasmid pBAD33 carries the *araBAD* promoter and the *araC* gene encoding the positive and negative regulator.[67] Plasmid pJY19 is a derivative of plasmid pTTQ18 (Amersham), and carries the *tac* promoter, the $lacI^q$ gene and the different multiple cloning site of

Table 1. Bacterial strains and plasmids used in this study

Strain or plasmid	Description	Source or reference
A. V. alginolyticus *strains*		
VIO5	Pof^+, Laf^-	31,47
YM4	Pof^+, Laf^-	46
YM14	Pof^-, Laf^-, *rpoN*	47
NMB107	Pof^-, Laf^-, *fliG*	This work
NMB196	Pof^-, Laf^-, Δ*fliF*	This work
NMB198	Pof^-, Laf^-, Δ*fliG*	This work
B. E. coli *strains*		
JM109		74
DFB225	Δ*fliG*	15
C. *Plasmids*		
pSU41	Km^r, P*lac lacZa*	66
pBAD33	Cm^r, P*BAD*	67
pJY19	Ap^r, P*tac lacZa*, $lacI^q$	This work
pEGFP	GFP expression vector	Clontech
pSL27	*E. coli* FliG in pAlter-1	15
pJN131	PomA and PomB in pJY19	This work
pAM101	*V. alginolyticus* FliG in pCR2.1	This work
pAM305	*V. alginolyticus* FliG in pSU41	This work
pTY101	*V. alginolyticus* FliG in pBAD33	This work
pTY102	*V. alginolyticus* FliG in pBAD33	This work
pTY200	GFP in pBAD33	This work
pTY201	GFP–FliG in pBAD33	This work
pTY202	FliG–GFP in pBAD33	This work
pTY301	*E. coli* FliG in pBAD33	This work
pTY401	$FliG^{VE}$ chimera in pBAD33	This work
pTY402	$FliG^{EV}$ chimera in pBAD33	This work
pTY501	*V. alginolyticus* FliF in pGEM-T Easy	This work
pTY601	*V. alginolyticus* FliF and FliG in pBAD33	This work
pTY602	*V. alginolyticus* FliF and $FliG^{VE}$ chimera in pBAD33	This work

Km^r, kanamycin resistant; Cm^r, chloramphenicol resistant; Ap^r, ampicillin resistant; P*lac*, *lac* promoter; P*tac*, *tac* promoter; P*BAD*, ara*BAD* promoter.

pTTQ18. The pAlter1 (Promega)-based plasmid, pSL27, carries the *E. coli fliG* gene, which was kindly provided by D.F. Blair.[68] Plasmid pEGFP encodes the enhanced green fluorescent protein (EGFP) (Clontech). For the production of FliG (i.e. FliG, GFP–FliG and FliG–GFP proteins) and GFP proteins in this study, the coding regions were placed downstream of the *araBAD* promoter on the vector pBAD33. Plasmid pTY401 carrying the FliG chimera was prepared by replacement of a *Sal*I-*Hin*dIII fragment of pTY102 containing the C-terminal region of the *V. alginolyticus fliG* gene with a *Sal*I-*Hin*dIII fragment of pTY301 containing the C-terminal region of the *E. coli fliG* gene. Plasmid pTY402 was prepared by replacement of a *Sal*I-*Hin*dIII fragment of pTY301, the C-terminal region of the *E. coli fliG* gene, with a *Sal*I-*Hin*dIII fragment of pTY102, the C-terminal region of the *V. alginolyticus fliG* gene.

Cloning *fliG* and *fliF* genes

The primers (5′-GCTCAAGTAGTGAAGAACTGGATGCA-3′ and 5′-TCCCGCACCGTAATCCGGNAGNCCCCA-3′) were synthesized from the genome sequence of *V. cholerae* and the *fliG* gene and surrounding sequences were amplified by PCR using *V. alginolyticus* VIO5 chromosomal DNA as the template. The 1.2 kb amplified fragment was cloned into pCR2.1 (Invitrogen), resulting pAM101, and the 1.2 kb *Sph*I-*Bam*HI fragment was subcloned into pSU41, resulting in plasmid pAM305.

For the *fliF* gene cloning, the primers (5′-GCCACTGTTCAAATCCGCAATAAGC-3′ and 5′-GCTCAACTGGCATTCCCGCG-3′) were synthesized based on sequences from *V. parahaemolyticus* and *V. alginolyticus*, respectively, and the *fliF* gene and surrounding sequences were amplified by PCR using *V. alginolyticus* VIO5 chromosomal DNA as the template. The 1.9 kb amplified fragment was cloned into pGEM-T Easy vector (Promega), resulting in pTY501. The cloned *fliG* and *fliF* genes were confirmed by DNA sequencing.

Construction of *fliF* and *fliG* deletion mutants

The *fliG* deletion mutant (NMB198) and the *fliF* deletion mutant (NMB196) were generated by homologous recombination using a suicide vector as described.[69] An in-frame deletion of *fliG* was constructed by using the three internal *Ava*II sites, resulting in the deletion of amino acid residues 55–175. An in-frame deletion of *fliF* was constructed by using the internal *Hin*dIII (filled in by T4 polymerase) and *Eco*RV sites, resulting in the deletion of amino acid residues 106–294. The deleted alleles were introduced into VIO5. Motility-defective mutants with resistance to chloramphenicol were selected first on semi-solid agar plates, and chloramphenicol-sensitive mutants were identified.

Site-directed mutagenesis

To introduce amino acid substitutions or a *Sal* I-digestion site into *fliG*, we used a previously described PCR method.[70] We synthesized pairs of mutant primers homologous to either the sense or antisense strand of the *fliG* gene, with a 1–3 base mismatch at the mutation site. We amplified the full plasmid sequence containing the *fliG* gene. The presence of the *fliG* mutations was confirmed by DNA sequencing.

Detection of FliG proteins

For immunoblotting, anti-FliG antibody, called αFliG2, was raised against a synthetic peptide (NH_2-PVELDVSTITGEEKA-COOH) corresponding to a partial sequence (Pro16 to Ala30) of *V. alginolyticus* FliG and affinity-purified as described.[71] *Vibrio* cells harboring a vector or plasmid encoding wild-type FliG or various FliG variants were cultured in VPG medium in the presence or absence of 1 mM L-arabinose and collected by centrifugation at mid-log phase. Collected cells were solubilized with SDS-sample buffer and subjected to SDS-12% PAGE followed by immunoblotting with antibody against GFP (Molecular Probe) or the FliG peptide.

Observation of the subcellular localization of GFP–FliG

NMB107 or YM14 cells carrying the pBAD33-based plasmids encoding GFP (pTY200), GFP–FliG (pTY201) or FliG–GFP (pTY202) were grown in VPG medium with 1 mM arabinose at 30 °C. At late exponential phase, a small aliquot of the cell suspension was spotted onto glass slides coated with 0.5% agarose and observed under a fluorescence microscope (Olympus, BX50), as described.[72] The images were recorded and processed by using a digital camera (Hamamatsu Photonics, C4742-95) and imaging software (Scanalytics, IP Lab ver. 3.2). For observation of GFP–FliG with the flagellum, NMB107 cells carrying plasmid encoding GFP–FliG (pTY201) were grown as described above. The cell suspension on the glass slide covered by a cover-glass with a spacer was washed twice with V-buffer (25 mM Tris–HCl (pH7.5), 10 mM $MgCl_2$, 300 mM NaCl) and reacted with V-buffer containing anti-polar flagellum (Pof) antibody. After washing with V-buffer, anti-rabbit IgG conjugated with rhodamine was applied and then washed with V-buffer. Cells on the cover-glass were observed in the microscope as described above.

Measurement of swimming speed

Cells were harvested at late logarithmic phase and suspended in TMN buffer (50 mM Tris–HCl (pH 7.5), 5 mM $MgCl_2$, 50 mM NaCl, 250 mM KCl). The cell suspension was diluted 100-fold in TMN buffer, and cells were observed at room temperature under a dark-field microscope and recorded on videotape. Their swimming speed was determined as described.[73]

Membrane preparation and protease treatment

The procedure for membrane preparation was basically as described by Sato & Homma.[34] JM109 cells harboring plasmids were grown in TB medium in the presence of arabinose until late-log phase. If necessary, IPTG was added to a final concentration of 1 mM. Harvested cells were suspended in lysis buffer (20 mM potassium phosphate (pH 8.0), 150 mM NaCl, 10 mM $MgSO_4$, 10% (w/v) glycerol) containing 30 μg/ml of DNase I and the suspension was passed twice through a French press at 4000 lb/in.^{2} Unbroken cells were removed by low-speed centrifugation, and the membrane pellet (P100) and the cytoplasm supernatant (S100) were recovered after centrifugation at 100,000*g* for one hour. The P100 fraction (membrane) was resuspended in lysis buffer, and the membrane proteins (0.5 mg/ml) were digested with trypsin or proteinase K

at the indicated concentrations on ice for 30 minutes. The samples were precipitated with trichloroacetic acid, washed with acetone, and then analyzed by SDS-PAGE, followed by immunoblotting with anti-FliG antibody.

Acknowledgements

We thank Dr D. F. Blair for providing plasmids and bacterial strains. This work was supported, in part, by grants-in-aid for scientific research from the Ministry of Education, Science and Culture of Japan (to M.H. and to T.Y.) and from the Japan Society for the Promotion of Science (to T.Y.).

References

1. Blair, D. F. (2003). Flagellar movement driven by proton translocation. *FEBS Letters*, **545**, 86–95.
2. Macnab, R. M. (1999). The bacterial flagellum: reversible rotary propellor and type III export apparatus. *J. Bacteriol.* **181**, 7149–7153.
3. Berg, H. C. (2003). The rotary motor of bacterial flagella. *Annu. Rev. Biochem.* **72**, 19–54.
4. Chun, S. Y. & Parkinson, J. S. (1988). Bacterial motility: membrane topology of the *Escherichia coli* MotB protein. *Science*, **239**, 276–278.
5. Zhou, J. D., Fazzio, R. T. & Blair, D. F. (1995). Membrane topology of the MotA protein of *Escherichia coli*. *J. Mol. Biol.* **251**, 237–242.
6. De Mot, R. & Vanderleyden, J. (1994). The C-terminal sequence conservation between OmpA-related outer membrane proteins and MotB suggests a common function in both Gram-positive and Gram-negative bacteria, possibly in the interaction of these domains with peptidoglycan. *Mol. Microbiol.* **12**, 333–334.
7. Koebnik, R. (1995). Proposal for a peptidoglycan-associating alpha-helical motif in the C-terminal regions of some bacterial cell-surface proteins. *Mol. Microbiol.* **16**, 1269–1270.
8. Khan, S., Dapice, M. & Reese, T. S. (1988). Effects of *mot* gene expression on the structure of the flagellar motor. *J. Mol. Biol.* **202**, 575–584.
9. Blair, D. F. & Berg, H. C. (1990). The MotA protein of *E. coli* is a proton-conducting component of the flagellar motor. *Cell*, **60**, 439–449.
10. Stolz, B. & Berg, H. C. (1991). Evidence for interactions between MotA and MotB, torque-generating elements of the flagellar motor of *Escherichia coli*. *J. Bacteriol.* **173**, 7033–7037.
11. Tang, H., Braun, T. F. & Blair, D. F. (1996). Motility protein complexes in the bacterial flagellar motor. *J. Mol. Biol.* **261**, 209–221.
12. Marykwas, D. L., Schmidt, S. A. & Berg, H. C. (1996). Interacting components of the flagellar motor of *Escherichia coli* revealed by the two-hybrid system in yeast. *J. Mol. Biol.* **256**, 564–576.
13. Yamaguchi, S., Fujita, H., Ishihara, H., Aizawa, S. & Macnab, R. M. (1986). Subdivision of flagellar genes of *Salmonella typhimurium* into regions responsible for assembly, rotation, and switching. *J. Bacteriol.* **166**, 187–193.
14. Yamaguchi, S., Aizawa, S., Kihara, M., Isomura, M., Jones, C. J. & Macnab, R. M. (1986). Genetic evidence for a switching and energy-transducing complex in the flagellar motor of *Salmonella typhimurium*. *J. Bacteriol.* **168**, 1172–1179.
15. Lloyd, S. A., Tang, H., Wang, X., Billings, S. & Blair, D. F. (1996). Torque generation in the flagellar motor of *Escherichia coli*: evidence of a direct role for FliG but not for FliM or FliN. *J. Bacteriol.* **178**, 223–231.
16. Francis, N. R., Irikura, V. M., Yamaguchi, S., DeRosier, D. J. & Macnab, R. M. (1992). Localization of the *Salmonella typhimurium* flagellar switch protein FliG to the cytoplasmic M-ring face of the basal body. *Proc. Natl Acad. Sci. USA*, **89**, 6304–6308.
17. Zhao, R. H., Pathak, N., Jaffe, H., Reese, T. S. & Khan, S. (1996). FliN is a major structural protein of the C-ring in the *Salmonella typhimurium* flagellar basal body. *J. Mol. Biol.* **261**, 195–208.
18. Derosier, D. J. (1998). The turn of the screw: the bacterial flagellar motor. *Cell*, **93**, 17–20.
19. Lloyd, S. A., Whitby, F. G., Blair, D. F. & Hill, C. P. (1999). Structure of the C-terminal domain of FliG, a component of the rotor in the bacterial flagellar motor. *Nature*, **400**, 472–475.
20. Brown, P. N., Hill, C. P. & Blair, D. F. (2002). Crystal structure of the middle and C-terminal domains of the flagellar rotor protein FliG. *EMBO J.* **21**, 3225–3234.
21. Imae, Y. & Atsumi, T. (1989). Na^+-driven bacterial flagellar motors. *J. Bioenerg. Biomembr.* **21**, 705–716.
22. Yorimitsu, T. & Homma, M. (2001). Na^+-driven flagellar motor of *Vibrio*. *Biochim. Biophys. Acta*, **1505**, 82–93.
23. McCarter, L. L. (2001). Polar flagellar motility of the *Vibrionaceae*. *Microbiol. Mol. Biol. Rev.* **65**, 445–462.
24. Kojima, S., Yamamoto, K., Kawagishi, I. & Homma, M. (1999). The polar flagella motor of *Vibrio cholerae* is driven by an Na^+ motive force. *J. Bacteriol.* **181**, 1927–1930.
25. Häse, C. C. & Mekalanos, J. J. (1999). Effects of changes in membrane sodium flux on virulence gene expression in *Vibrio cholerae*. *Proc. Natl Acad. Sci. USA*, **96**, 3183–3187.
26. Zhou, J., Sharp, L. L., Tang, H. L., Lloyd, S. A., Billings, S., Braun, T. F. & Blair, D. F. (1998). Function of protonatable residues in the flagellar motor of *Escherichia coli*: a critical role for Asp 32 of MotB. *J. Bacteriol.* **180**, 2729–2735.
27. Asai, Y., Kojima, S., Kato, H., Nishioka, N., Kawagishi, I. & Homma, M. (1997). Putative channel components for the fast-rotating sodium-driven flagellar motor of a marine bacterium. *J. Bacteriol.* **179**, 5104–5110.
28. Kojima, S. & Blair, D. F. (2001). Conformational change in the stator of the bacterial flagellar motor. *Biochemistry*, **40**, 13041–13050.
29. McCarter, L. L. (1994). MotY, a component of the sodium-type flagellar motor. *J. Bacteriol.* **176**, 4219–4225.
30. McCarter, L. L. (1994). MotX, the channel component of the sodium-type flagellar motor. *J. Bacteriol.* **176**, 5988–5998.
31. Okunishi, I., Kawagishi, I. & Homma, M. (1996). Cloning and characterization of *motY*, a gene coding for a component of the sodium-driven flagellar motor in *Vibrio alginolyticus*. *J. Bacteriol.* **178**, 2409–2415.
32. Okabe, M., Yakushi, T., Asai, Y. & Homma, M. (2001). Cloning and characterization of *motX*, a *Vibrio alginolyticus* sodium-driven flagellar motor gene. *J. Biochem.* **130**, 879–884.
33. Okabe, M., Yakushi, T., Kojima, M. & Homma, M.

(2002). MotX and MotY, specific components of the sodium-driven flagellar motor, colocalize to the outer membrane in *Vibrio alginolyticus*. *Mol. Microbiol.* **46**, 125–134.
34. Sato, K. & Homma, M. (2000). Functional reconstitution of the Na^+-driven polar flagellar motor component of *Vibrio alginolyticus*. *J. Biol. Chem.* **275**, 5718–5722.
35. Sato, K. & Homma, M. (2000). Multimeric structure of PomA, the Na^+-driven polar flagellar motor component of *Vibrio alginolyticus*. *J. Biol. Chem.* **275**, 20223–20228.
36. Yorimitsu, T., Sato, K., Asai, Y. & Homma, M. (2000). Intermolecular cross-linking between the periplasmic $loop_{3-4}$ regions of PomA, a component of the Na^+-driven flagellar motor of *Vibrio alginolyticus*. *J. Biol. Chem.* **275**, 31387–31391.
37. Braun, T. F. & Blair, D. F. (2001). Targeted disulfide cross-linking of the MotB protein of *Escherichia coli*: evidence for two H^+ channels in the stator complex. *Biochemistry*, **40**, 13051–13059.
38. Asai, Y., Kawagishi, I., Sockett, E. & Homma, M. (1999). Hybrid motor with the H^+-and Na^+-driven components can rotate *Vibrio* polar flagella by using sodium ions. *J. Bacteriol.* **181**, 6322–6338.
39. Asai, Y., Sockett, R. E., Kawagishi, I. & Homma, M. (2000). Coupling ion specificity of chimeras between H^+- and Na^+-driven motor proteins, MotB and PomB, in *Vibrio* polar flagella. *EMBO J.* **19**, 3639–3648.
40. Asai, Y., Yakushi, T., Kawagishi, I. & Homma, M. (2003). Ion-coupling determinants of Na^+-driven and H^+-driven flagellar motors. *J. Mol. Biol.* **327**, 453–463.
41. Sowa, Y., Hotta, H., Homma, M. & Ishijima, A. (2003). Torque–speed relationship of the Na^+-driven flagellar motor of *Vibrio alginolyticus*. *J. Mol. Biol.* **327**, 1043–1051.
42. Zhou, J. D., Lloyd, S. A. & Blair, D. F. (1998). Electrostatic interactions between rotor and stator in the bacterial flagellar motor. *Proc. Natl Acad. Sci. USA*, **95**, 6436–6441.
43. Lloyd, S. A. & Blair, D. F. (1997). Charged residues of the rotor protein FliG essential for torque generation in the flagellar motor of *Escherichia coli*. *J. Mol. Biol.* **266**, 733–744.
44. Zhou, J. D. & Blair, D. F. (1997). Residues of the cytoplasmic domain of MotA essential for torque generation in the bacterial flagellar motor. *J. Mol. Biol.* **273**, 428–439.
45. Yorimitsu, T., Sowa, Y., Ishijima, A., Yakushi, T. & Homma, M. (2002). The systematic substitutions around the conserved charged residues of the cytoplasmic loop of Na^+-driven flagellar motor component PomA. *J. Mol. Biol.* **320**, 403–413.
46. Kawagishi, I., Maekawa, Y., Atsumi, T., Homma, M. & Imae, Y. (1995). Isolation of the polar and lateral flagellum-defective mutants in *Vibrio alginolyticus* and identification of their flagellar driving energy sources. *J. Bacteriol.* **177**, 5158–5160.
47. Kawagishi, I., Nakada, M., Nishioka, N. & Homma, M. (1997). Cloning of a *Vibrio alginolyticus rpoN* gene that is required for polar flagellar formation. *J. Bacteriol.* **179**, 6851–6854.
48. Allen, R. D. & Baumann, P. (1971). Structure and arrangement of flagella in species of the genus *Beneckea* and *Photobacterium fischeri*. *J. Bacteriol.* **107**, 295–302.
49. Gosink, K. K. & Häse, C. C. (2000). Requirements for conversion of the Na^+-driven flagellar motor of *Vibrio cholerae* to the H^+-driven motor of *Escherichia coli*. *J. Bacteriol.* **182**, 4234–4240.
50. Kubori, T., Yamaguchi, S. & Aizawa, S. (1997). Assembly of the switch complex onto the MS ring complex of *Salmonella typhimurium* does not require any other flagellar proteins. *J. Bacteriol.* **179**, 813–817.
51. Irikura, V. M., Kihara, M., Yamaguchi, S., Sockett, H. & Macnab, R. M. (1993). *Salmonella typhimurium fliG* and *fliN* mutations causing defects in assembly, rotation, and switching of the flagellar motor. *J. Bacteriol.* **175**, 802–810.
52. Marykwas, D. L. & Berg, H. C. (1996). A mutational analysis of the interaction between FliG and FliM, two components of the flagellar motor of *Escherichia coli*. *J. Bacteriol.* **178**, 1289–1294.
53. Sourjik, V. & Berg, H. C. (2000). Localization of components of the chemotaxis machinery of *Escherichia coli* using fluorescent protein fusions. *Mol. Microbiol.* **37**, 740–751.
54. Hess, J. F., Oosawa, K., Kaplan, N. & Simon, M. I. (1988). Phosphorylation of three proteins in the signaling pathway of bacterial chemotaxis. *Cell*, **53**, 79–87.
55. Borkovich, K. A., Kaplan, N., Hess, J. F. & Simon, M. I. (1989). Transmembrane signal transduction in bacterial chemotaxis involves ligand-dependent activation of phosphate group transfer. *Proc. Natl Acad. Sci. USA*, **86**, 1208–1212.
56. Barak, R. & Eisenbach, M. (1992). Correlation between phosphorylation of the chemotaxis protein CheY and its activity at the flagellar motor. *Biochemistry*, **31**, 1821–1826.
57. Welch, M., Oosawa, K., Aizawa, S. I. & Eisenbach, M. (1993). Phosphorylation-dependent binding of a signal molecule to the flagellar switch of bacteria. *Proc. Natl Acad. Sci. USA*, **90**, 8787–8791.
58. Noji, H., Yasuda, R., Yoshida, M. & Kinosita, K. J. (1997). Direct observation of the rotation of F_1-ATPase. *Nature*, **386**, 299–302.
59. Hara, K. Y., Noji, H., Bald, D., Yasuda, R., Kinosita, K., Jr & Yoshida, M. (2000). The role of the DELSEED motif of the β subunit in rotation of F_1-ATPase. *J. Biol. Chem.* **275**, 14260–14263.
60. Hara, K. Y., Kato-Yamada, Y., Kikuchi, Y. & Hisabori, T. M. Y. (2001). The role of the βDELSEED motif of F_1-ATPase. *J. Biol. Chem.* **276**, 23969–23973.
61. Tsunoda, S. P., Rodgers, A. J., Aggeler, R., Wilce, M. C., Yoshida, M. & Capaldi, R. A. (2001). Large conformational changes of the ε subunit in the bacterial F_1F_0 ATP synthase provide a ratchet action to regulate this rotary motor enzyme. *Proc. Natl Acad. Sci. USA*, **98**, 6560–6564.
62. Braun, T. F., Poulson, S., Gully, J. B., Empey, J. C., Van, W. S., Putnam, A. & Blair, D. F. (1999). Function of proline residues of MotA in torque generation by the flagellar motor of *Escherichia coli*. *J. Bacteriol.* **181**, 3542–3551.
63. Magariyama, Y., Sugiyama, S., Muramoto, K., Maekawa, Y., Kawagishi, I., Imae, Y. & Kudo, S. (1994). Very fast flagellar rotation. *Nature*, **381**, 752.
64. Lowe, G., Meister, M. & Berg, H. C. (1987). Rapid rotation of flagellar bundles in swimming bacteria. *Nature*, **325**, 637–640.
65. Sambrook, J., Fritsch, E. F. & Maniatis, T. (1989). *Molecular Cloning: A Laboratory Manual*, 2nd edit., Cold Spring Habor Laboratory Press, Plainview, NY.
66. Bartolome, B., Jubete, Y., Martínez, E. & de la Cruz, F. (1991). Construction and properties of a family of

pACYC184-derived cloning vectors compatible with pBR322 and its derivatives. *Gene*, **102**, 75–78.
67. Guzman, L. M., Belin, D., Carson, M. J. & Beckwith, J. (1995). Tight regulation, modulation, and high-level expression by vectors containing the arabinose pBAD promoter. *J. Bacteriol.* **177**, 4121–4130.
68. Tang, H. & Blair, D. F. (1995). Regulated underexpression of the FliM protein of *Escherichia coli* and evidence for a location in the flagellar motor distinct from the MotA;MotB torque generators. *J. Bacteriol.* **177**, 3485–3495.
69. Xu, M., Yamamoto, K., Honda, T. & Ming, X. (1994). Construction and characterization of an isogenic mutant of *Vibrio parahaemolyticus* having a deletion in the thermostable direct hemolysin-related hemolysin gene (*trh*). *J. Bacteriol.* **176**, 4757–4760.
70. Kojima, S., Asai, Y., Atsumi, T., Kawagishi, I. & Homma, M. (1999). Na^+-driven flagellar motor resistant to phenamil, an amiloride analog, caused by mutations of putative channel components. *J. Mol. Biol.* **285**, 1537–1547.
71. Yorimitsu, T., Sato, K., Asai, Y., Kawagishi, I. & Homma, M. (1999). Functional interaction between PomA and PomB, the Na^+-driven flagellar motor components of *Vibrio alginolyticus*. *J. Bacteriol.* **181**, 5103–5106.
72. Shiomi, D., Zhulin, I. B., Homma, M. & Kawagishi, I. (2002). Dual recognition of the bacterial chemoreceptor by chemotaxis-specific domains of the CheR methyltransferase. *J. Biol. Chem.* **277**, 42325–42333.
73. Atsumi, T., Maekawa, Y., Yamada, T., Kawagishi, I., Imae, Y. & Homma, M. (1996). Effect of viscosity on swimming by the lateral and polar flagella of *Vibrio alginolyticus*. *J. Bacteriol.* **178**, 5024–5026.
74. Yanisch-Perron, C., Vieira, J. & Messing, J. (1985). Improved M13 phage cloning vectors and host strains: nucleotide sequences of the M13mp18 and pUC19 vectors. *Gene*, **33**, 103–119.

Edited by J. Karn

(Received 14 July 2003; received in revised form 23 September 2003; accepted 25 September 2003)